

# DAMPING STRATEGIES FOR ENERGY EFFICIENT PRESSURE CONTROLLERS OF VARIABLE DISPLACEMENT PUMPS

Florian Schoemacker\*, Felix Fischer, Katharina Schmitz

*Institute for Fluid Power Drives and Systems, RWTH Aachen University, Campus-Boulevard 30, 52074 Aachen*

\* Corresponding author: Tel.: +49 241 8047748; E-mail address: [florian.schoemacker@ifas.rwth-aachen.de](mailto:florian.schoemacker@ifas.rwth-aachen.de)

## ABSTRACT

In hydraulic-mechanically controlled variable displacement pumps, the actual pump controller produces additional power losses. Due to the low damping coefficients of all pump controller's components, hydraulic-mechanically pressure controlled pumps use to oscillate while adjusting the pressure level in the hydraulic system. In several state-of-the-art variable pump controllers, a damping orifice connects the control actuator's displacement chamber with the reservoir. This bypass dampens the movement of the control actuator but also leads to bypass losses during steady-state operation of the pump. A new concept for damping via feedback loops avoiding bypass losses is presented in this paper.

*Keywords:* Variable displacement pumps, Axial piston pumps, Pressure controller, Feedback loops

## 1. INTRODUCTION

The system "hydraulic variable displacement pump" consists of mainly two components. One is the pump itself with the cylinder block, pistons, valve plate and swash plate. The other part is the pump controller including the control valve and control actuators. The design of the pump controller depends on the function of the pump system, for example pressure compensation or flow control. In order to change the output flow rate, the pump controller acts on the swash plate via the control piston. This results in a change of the swash plate angle and the displacement volume, which determines the output flow.

During steady-state operation, the force of the control piston is in equilibrium with the torque load of the piston pressure forces and spring forces acting on the swash plate.

The scheme of a pressure controlled pump system is shown in **Figure 1**. For this study, the control piston is equipped with two pressurized areas. The smaller ring area is connected to the high pressure port of the pump. The opposing area is part of the control actuator's displacement chamber and applied with the control pressure, which is supplied by the pump controller.

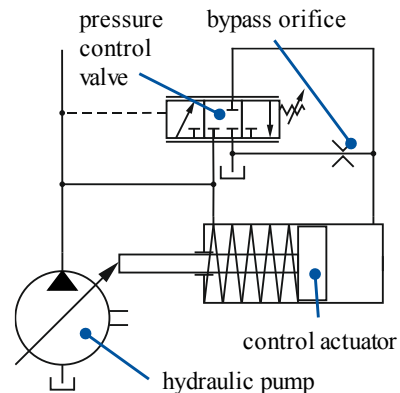


**Figure 1:** Pump system with hydraulic-mechanical pressure controller

In variable displacement pumps, the actual pump controller produces additional power losses. Due to the low damping coefficients of all the pump controller's components, pressure controlled pumps use to oscillate while adjusting the pressure level in the hydraulic system. In several state-of-the-art pump controllers, a damping orifice connects the control actuator's displacement chamber with the reservoir. This bypass dampens the movement of the control actuator, but also leads to bypass losses during steady-state operation of the pump.

The bypass-losses of the orifice have been measured in this study, see **Figure 2**. The typical control pressure yields to 70 bar. This value is valid for a control actuator with an area ratio of 1:4 and a system pressure level of 300 bar. At this operating point, a flow of 1.66 l/min occurs.

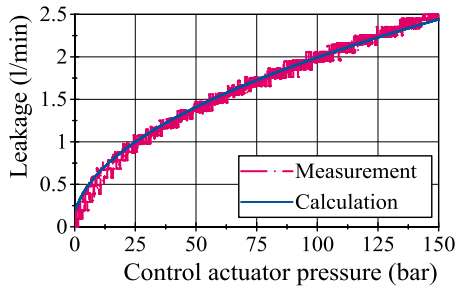


**Figure 2:** Characteristic curve of the flow via the bypass orifice

For controlling a pump pressure level of 300 bar, the power loss of the orifice results in 0.85 kW, see Eq. 1. The bypass losses are fed by the high pressure port of the pump.

$$P_{\text{Loss}} = p_{\text{HP}} \cdot Q_{\text{Bypass}} = 0,85 \text{ kW} \quad (1)$$

These bypass losses occur continuously during the operation of the pump and are only influenced by the system pressure, which has an impact on the control actuator's pressure.

In addition to the loss of the bypass orifice, losses at the pressure control valve occur. The overall power consumption of the pump controller is shown in **Figure 3** as a percentage of the hydraulic output power, because the necessary volume flow is taken from the output flow rate of the pump. The pressure level is 300 bar and the maximum power output 35 kW.

The red line is the result of a measurement of a state-of-the-art pump controller [7]. The percentage is increased at lower swash plate angle, because the hydraulic output power is reduced but the power consumption of the pump controller do not vary.

Using an electro hydraulic pump controller the power consumption can be reduced by about 70 %. The goal of this research is to develop a pump controller without continuous bypass losses.

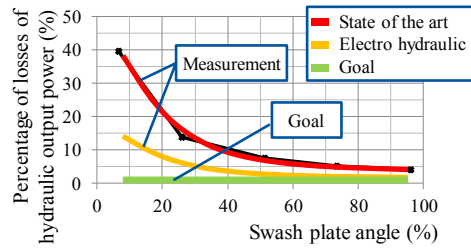


**Figure 3:** Power consumption of pump controllers as percentage of hydraulic output power

### 1.1. State of the art

Dreymüller [1] investigated the dynamic behaviour of hydraulic-mechanical pump controllers. The connection of the high pressure port to the ring area of the control actuator results in pressure pulsations. Dreymüller suggests that the pressure signal should be dampened before fed to the pressure control valve. Furthermore, Dreymüller shows the necessity of a system dampening of the pump controller, for example via the bypass orifice.

Murrenhoff [2] focused in his research on the control strategy for hydraulic motors. Motor controllers are able to control speed or torque output, but the architecture is similar to pump controllers. Murrenhoff showed that a controller can be dampened using a mechanical feedback loop.

Langen [3] compared hydraulic-mechanical to electrohydraulic pump controllers. For the electrohydraulic controller, the system pressure is measured electronically. The controller then forwards the control signal to an electrohydraulic valve, which determines the volume flow to the control actuator. Langen used this electronic system architecture to verify the function of the feedback controller described in this paper. Furthermore, Langen carried out a parameter study of the control actuator's geometry and found the optimum of the area ratio at 1:4.

For the simulation of the swash plate oscillations, a detailed model of the pressure built-up dynamics during commutation as well as a pump controller model is needed. Manring and Johnson [4] published a mathematical description of the model for a variable displacement pump. Manring [5] also studied the forces acting on the swash plate and their variation due to the odd number of pistons. For

the simulation of a controlled pump, Mandal et al. [6] developed a model of the pressure compensator for a variable displacement pump. The model was used for designing the pump controller according to the dynamics of the swash plate.

Lux [7] experimentally investigated the losses of pump controllers. He measured the flow rate needed for the pump controller during operation of the pump, showing an efficiency reduction of pumps in closed-loop control. The power loss is almost constant for all swash plate angles but differs with the pressure level.

The presented literature deals with the investigation of the dynamics and the power loss of pump controllers. As an improvement of state-of-the-art pump controllers, the authors propose an innovative pump controller, which uses its system architecture instead of the bypass orifice in order to dampen the control actuator.

## 2. NEW SYSTEM ARCHITECTURE FOR PUMP CONTROLLERS

The new concept is based on feedback loops within the pump controller. These feedbacks result in a systematic damping of the pump controller and avoid unnecessary bypass losses. The possible power saving is greater than it could be obtained with an optimization of pump's tribological contacts [7].

In order to dampen the pressure oscillation of a variable displacement pump, the pump's output flow rate needs to be fed back to the pressure controller, because the output flow is the rate of change for the pressure of the hydraulic system. This concept of damping is known from damped harmonic oscillators. The position of the control actuator is proportional to the pump's output flow rate. Therefore, feedback loops are used to signal the change of the actuator's position to the pressure control valve in order to create an additional closed loop control within the pressure control loop. The design of feedback loops, which use this intention, are shown in the following.

The current position of the actuator can be fed back mechanically to the valve using a spring. This concept has already been proposed by Murrenhoff [2] and experimentally validated.

However, this results in an error in steady-state operation. An additional damper, which moves relatively between the spring and the valve's

spool, consumes the force with time and prevents an error in the closed-loop control. Therefore, the feedback loop acts as a derivative element with first-order lag.

A pump controller with this new system architecture is shown in **Figure 4**.

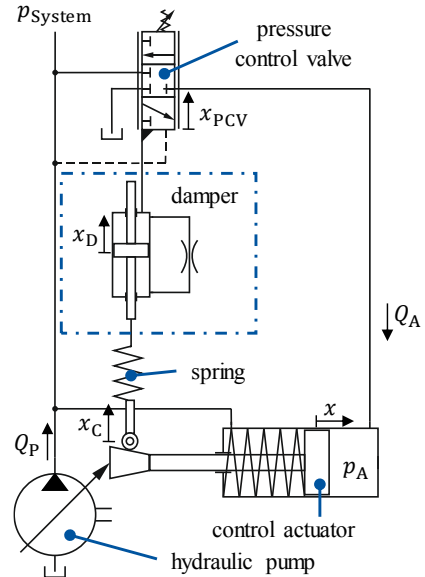


**Figure 4:** New concept with mechanical feedback of the control actuator's stroke

The function and the usability of systems built-up of derivative elements with first-order lag have been investigated by Luhmer [10] and Weingarten [11]. Their focus laid on the design of hydraulic circuits with this kind of function.

Applying their research, the same control scheme can be designed with hydraulic feedback in order to avoid a strict mechanical coupling between the control actuator and the valve's spool.

The hydraulic design of the concept is shown in **Figure 5**.

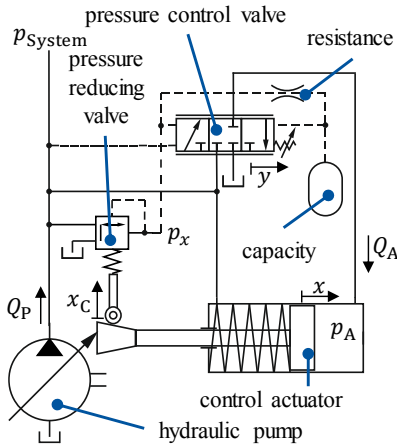


**Figure 5:** New concept with hydraulic feedback of the control actuator’s stroke

The presented concepts are investigated via simulation. This simulation is made up of an already existing pump model, which provides the control forces by calculating the pressure build-up for all pistons and deriving the torque load of the swash plate, combined with the model of an actual pump controller. Furthermore, the feedback loops are included in the model. The simulation results state the dynamics of the control system and the power losses. These are compared to state of the art pump controllers.

### 3. GEOMETRY AND SIMULATION MODEL

In the following, the geometry of the pump and the controller are presented and the simulation model is described. For the analysis, a swash plate-type axial piston pump has been chosen as a variable displacement controlled pump. The pump controller type is a pressure compensator, which adjusts the output flow according to the hydraulic system’s need in order to hold constant pressure. The pump’s geometric data is derived from an axial piston pump with a power output of about 30 kW. **Figure 6** shows the assembly of the pump system and a sketch of the hydraulic system used for displacement control. Forces acting on the swash plate are displayed as well.

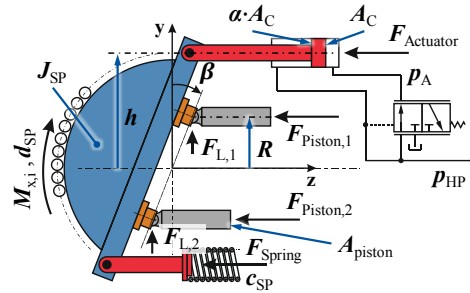


**Figure 6:** Pump system with pressure compensator [8]

The piston pressure forces act on the swash plate creating a periodically changing torque load. A spring provides the swash plate with an initial torque load for swiveling out, if the pump is in unpressurized condition. The torque load on the swash plate is balanced by the control actuator’s force. The actuator is supplied by the pump controller, which changes the swash plate angle in control operation.

For the simulation of the pump controllers with additional feedback loops, a lumped parameter model is used within the simulation software DSHplus. The pump model consists of the piston assembly’s mathematical description and its commutation to the high and low pressure kidney. The model is validated using the state of the art pressure controller.

The simulation model in DSHplus is shown in **Figure 7**.

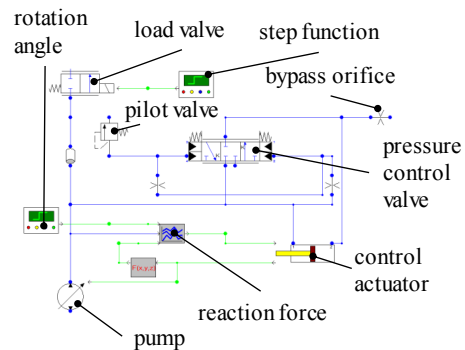


**Figure 7:** Model in DSHplus

The model contains the time behaviour of all components, which are necessary to simulate the dynamic response of the pump controller.

The control actuator is in equilibrium with the torque load on the swash plate. The torque load is

calculated using a complex model containing the pressure built up at each piston. The resulting forces are fed to the lumped parameter model using characteristic curves. The calculation is described in detail in chapter 3.1.

The characteristic curve of the valve within the pump controllers is obtained from the measurement of the volume flow via a real pump controller's valve.

Furthermore, the model needs to be completed with the new feedback loops. This description is presented in chapters 3.2 and 3.3.

### 3.1. Torque load

The simulation model is used as in [8]. In this model, the pressure built up of each piston of a nine piston pump according to its commutation with the valve plate is calculated. The commutation between piston chamber and valve plate opening is smoothed using silencing grooves. With the known pressure force of all pistons, the torque load of each piston and the resulting torque on the swash plate can be determined.

The mathematical calculation is based upon a Cartesian coordinate system, which is shown on **Figure 6**. The piston stroke of piston number  $i$  is given via Eq. 2.

$$s_i = R \cdot \tan(\beta) \cdot \sin(\varphi_i) \tag{2}$$

The torque load of each piston can be calculated using Eq. 3.

$$M_{x,i} = R \cdot (1 + \tan^2(\beta)) \cdot A_{\text{piston}} \cdot p_{i(\varphi_i)} \cdot \sin(\varphi_i) \tag{3}$$

The sum of all the piston's torque load is shown in **Figure 8** for one revolution of the pump.

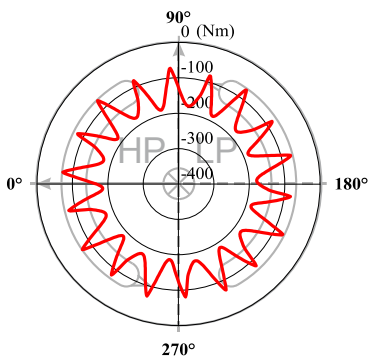


**Figure 8:** Torque load for one revolution [8]

In addition to the piston pressure forces, the spring and actuator forces act on the swash plate. Finally, the angle and angular velocity of the swash plate are determined using Euler's laws of motion (Eq. 4).

$$J_{SP} \cdot \ddot{\beta} + d_{SP} \cdot \dot{\beta} + c_{SP} \cdot \beta = \sum M_{x,i} + h \cdot A_C \cdot (\alpha \cdot p_{HP} - p_A) \tag{4}$$

The resulting force acting on the control actuator is calculated for different pressure, speeds and swash plate angles. The values are saved in characteristic curves and then fed to the lumped parameter model.

### 3.2. Mechanical feedback

For the mechanical feedback, a spring and a damper are installed between the control actuator and the pump controller. The components of the feedback loop are shown in **Figure 9**.

An additional spring  $c_{HD}$  assures that the pin is always in contact with the control actuator. The two springs  $c_{MF}$  allow the mechanical feedback to work in both directions.

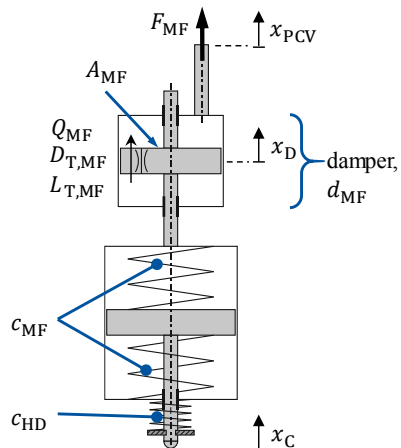


**Figure 9:** Mechanical feedback composed of spring and damper

The force feedback can be calculated using a mathematical description for the components. The equation of the spring damper with first order lag is given below. For the simulation, components with geometry parameters are implemented to show the impact of pressure built up in the damper. The variables  $x_C$ ,  $x_D$  and  $x_{PCV}$  are absolute values.

$$F_{MF} = c_{MF} \cdot (x_C - x_D) \quad (5)$$

$$F_{MF} = d_{MF} \cdot (\dot{x}_D - \dot{x}_{PCV}) \quad (6)$$

Deriving Eq. 5 and combining the results with Eq. 6 leads to the differential equation for the spring-damper system in Eq. 7.

$$\frac{d_{MF}}{c_{MF}} \cdot \dot{F}_{MF} + F_{MF} = d_{MF} \cdot (\dot{x}_C - \dot{x}_{PCV}) \quad (7)$$

The damper coefficient determines the time behaviour, whereas the spring coefficient gives the value of the momentum. The damper coefficient can be calculated using the flow rate equilibrium of the throttle and the cylinder.

$$Q_{MF} = A_{MF} \cdot (\dot{x}_D - \dot{x}_{PCV}) = \frac{\pi \cdot D_{T,MF}^4}{128 \cdot \eta \cdot l_{T,MF}} \cdot \frac{F_{MF}}{A_{MF}} \\ \Rightarrow d_{MF} = \frac{F_{MF}}{\dot{x}_D - \dot{x}_{PCV}} = \frac{\pi \cdot D_{T,MF}^4}{128 \cdot \eta \cdot l_{T,MF} \cdot A_{MF}^2} \quad (8)$$

The damping coefficient is independent from the velocity. Previous simulations have shown that the flow rate of the damper cylinder is too small to use an orifice instead of a throttle for the resistance. The diameter of the orifice would need to be smaller than 0.2 mm, which is inconvenient for manufacturing.

### 3.3. Hydraulic feedback

The hydraulic feedback uses a pressure signal proportional to the control actuator's stroke.

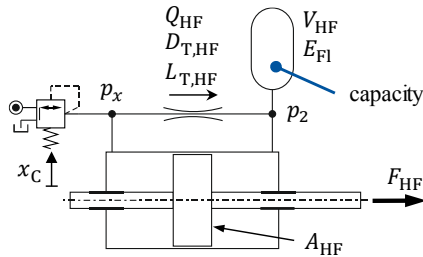


**Figure 10:** Hydraulic feedback composed of pressure valve

Pressure  $p_x$  is proportional to the control actuator's stroke. The time behaviour of the resulting force of the pressure difference due to the delayed pressure built up can be calculated using the following equation.

$$\dot{F}_{HF} = A_{HF} \cdot (\dot{p}_x - \dot{p}_2) = A_{HF} \cdot \left( K_{PRV} \cdot \dot{x}_C - \frac{E_{Fl}}{V_{HF}} \cdot \left( \frac{\pi \cdot D_{T,HF}^4}{128 \cdot \eta \cdot l_{T,HF}} \cdot \frac{F_{HF}}{A_{HF}} \right) \right) \quad (9)$$

This leads to the following equation.

$$\frac{V_{HF} \cdot 128 \cdot \eta \cdot l_{T,HF}}{E_{Fl} \cdot \pi \cdot D_{T,HF}^4} \cdot \dot{F}_{HF} + F_{HF} = A_{HF} \cdot K_{PRV} \cdot \frac{V_{HF} \cdot 128 \cdot \eta \cdot l_{T,HF}}{E_{Fl} \cdot \pi \cdot D_{T,HF}^4} \cdot \dot{x}_C \quad (10)$$

The time behaviour depends on the volume of the accumulator and the geometry of the throttle. As said for the mechanical feedback, an orifice cannot be used for the resistance, because of the marginal flow rate.

## 4. CRITERIA FOR COMPARISON

In order to compare the new pump controllers to the state of the art, criteria for the dynamics and the power loss are defined.

### 4.1. Dynamics

For the dynamic response, a rapid change in the volume flow demand is simulated using a step function. From the results, the time delay for reaching a certain pressure level can be compared. The dynamic response is shown in **Figure 11**.

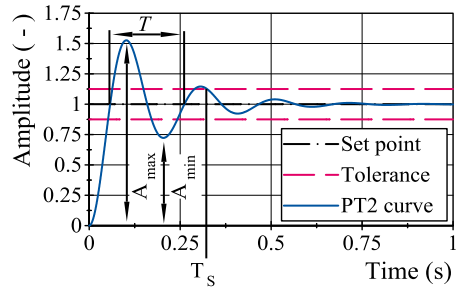


**Figure 11:** Dynamic response to a step function

**Figure 11** displays several resulting values describing the dynamics of the oscillation.  $A_{max}$  and  $A_{min}$  are the maximum and minimum amplitude and  $T$  is the period of the oscillation.

The curve reaches a tolerance band, which is deliberately defined. The settling time  $T_s$  is the point, at which the curve does not leave the tolerance band again [12]. For the discussion of the simulation results, the value of  $T_s$  is used.

### 4.2. Power loss

The power loss for each pressure controller is calculated in the simulation. This is the entire

volume flow taken from the output flow and going into the pump controller.

The mechanical feedback loop increases the load of the control actuator due to force feedback and the friction within the damper. Therefore, the control pressure increases, which leads to lower volume flow into the actuator and slower response of the pump controller. Thus, by the chosen power loss definition, friction in the damper is not accounted as a power loss but a decrease in dynamics.

The hydraulic feedback loop requires additional hydraulic power, which is added to the power loss of the pump controller.

## 5. RESULTS

The two principles for the feedback are compared to the state of the art. In order to do so, the state of the art pump controller is validated at first.

### 5.1. Validation of the state of the art pressure controller

The response to a step from 0.5 to 0.75 of the maximum flow rate is shown in **Figure 12** for the simulation and the measurement.

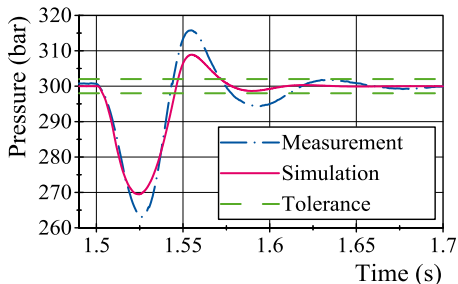


**Figure 12:** Dynamic response of the state of the art pump controller

The period of the two results match, but the amplitude of the measurement is higher than of the simulation results. This means, that the damping within the simulation model is higher than in reality. Concluding, the simulation model is sufficiently validated and can be used to calculate the pressure controller with additional feedback loops.

The continuous power loss is about 1.18 kW. This includes losses of the bypass orifice as well as the loss of the pressure control valve. For the comparison of the dynamics of the pump

controller, the value of settling time  $T_S$  of the state-of-the-art controller is set to 100 %.

### 5.2. Mechanical feedback

The dynamic response of the mechanical feedback is shown in **Figure 13**. The curves allow a comparison between the mechanical feedback and the state of the art pump controller, and an ideal first order lag feedback. This shows the influence of disturbances, as e.g. inertia and friction in the mechanical parts.

The ideal DT1 curve represents the feedback via a DT1 element. The parameters have been obtained via an optimization towards the smallest error of the curve compared to the set point. These parameters do not necessarily represent the very ideal solution according to the damping.

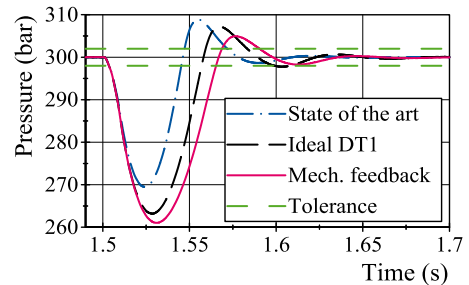


**Figure 13:** Dynamic response of the mechanical feedback loop

For the dynamics, the response of the mechanical feedback to the step function is a little bit slower and so the pressure drop of the system is larger. The delay is quantified by the settling time  $T_S$ , which is 25 % longer compared to the state-of-the-art pump controller.

The power loss of the pump controller with mechanical feedback is reduced to 0.64 kW. This is only 55 % of the power loss of the state-of-the-art pump controller. The reduction results from avoiding the losses of the bypass valve. But the volume loss of the pressure control valve rises due to an altered operation point. Within the state-of-the-art pump controller, the bypass leakage has to pass the valve first. Because this volume flow is avoided, the opening of the valve during steady-state operation is changed.



### 5.3. Hydraulic feedback

The dynamic response of the hydraulic feedback is shown in **Figure 14**. The hydraulic feedback can also be compared to the curve of the ideal DT1 feedback, which is the same as in **Figure 13**.

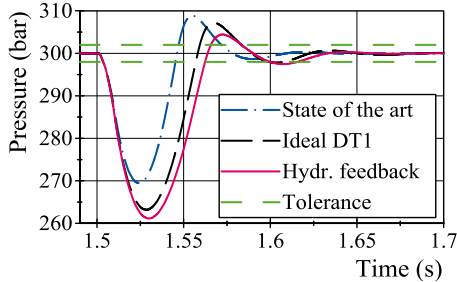


**Figure 14:** Dynamic response of the hydraulic feedback loop

The pump controller with hydraulic feedback is able to follow the curve of the DT1 feedback slightly better. The dynamic response is better than of the mechanical feedback with a value of the settling time  $T_S$ , which is only 15 % longer compared to the state-of-the-art pump controller.

For the hydraulic feedback, the necessary flow rate to pressurize the feedback loop is taken from the high-pressure port as well. Therefore, an additional power loss occurs. The power loss of the hydraulic feedback is reduced to 0.64 kW to the same value as of the mechanical feedback. Again, this is 55 % of the state-of-the-art pump controller's power loss.

## 6. CONCLUSION AND OUTLOOK

Several state-of-the-art hydraulic-mechanical pump pressure controllers are designed with a bypass orifice for the purpose of damping the pump controller. This leads to continuous bypass-losses, which are within the range of 1 kW and which are not ecological and economical reasonable anymore. Depending on the swash plate angle and the current hydraulic output power, the bypass losses are in the range of 3 to 40 % of the hydraulic output power.

Using a pump controller with an additional feedback loop as a damping strategy reduces the power loss of the entire system, consisting of pump and controller. For this purpose, concepts of pump controllers using mechanical and hydraulic feedback loops have been developed.

Simulation of the two concepts show that damping via this kind of systematic approach is

possible. Compared to the state-of-the-art pump controller, the bypass leakage can be avoided. The dynamic response of the concepts is slightly decreased. Comparing the power loss and the dynamics, the pump controller with hydraulic feedback represents a reasonable compromise.

The benefit using this new system architecture is cost reduction for operating the pump. This is an advantage for both, the pump manufacturer and the customer. Furthermore, the efficiency of the entire pump system is closer to the efficiency of the actual displacement part due to avoiding unnecessary bypass-losses.

### 6.1. Outlook

Within the scope of the research project, an experimental validation of the two concepts will also be performed. This will be done using a test bench, which allows to apply the same step function as a load upon the system. Furthermore, the pump controller will be investigated concerning the aspect of robustness against temperature change or particles.



## ACKNOWLEDGEMENT

The IGF research project 19789 N / 1 of the research association Forschungskuratorium Maschinenbau e. V. – FKM, Lyoner Straße 18, 60528 Frankfurt am Main was supported from the budget of the Federal Ministry of Economic Affairs through the AiF within the scope of a program to support industrial community research and development (IGF) based on a decision of the German Bundestag.

## NOMENCLATURE

$A_C$	Area of control actuator
$A_{HF}$	Area of cylinder in hydraulic feedback
$A_{MF}$	Area of damper cylinder
$A_{piston}$	Area of piston
$c_{MF}$	Spring coefficient of mechanical feedback
$c_{SP}$	Spring coefficient of swash plate
$D_{T,MF}$	Diameter of throttle in mechanical feedback
$D_{T,HF}$	Diameter of throttle in hydraulic feedback
$d_{MF}$	Damping coefficient of mechanical feedback
$d_{SP}$	Damping coefficient of swash plate
$E_{Fl}$	Bulk modulus
$F_{HF}$	Force of hydraulic feedback
$F_{MF}$	Force of mechanical feedback
$h$	Level arm
$J_{SP}$	Inertia of swash plate
$K_{PCV}$	Coefficient of pressure reducing valve
$L_{T,MF}$	Length of throttle in mechanical feedback
$L_{T,HF}$	Length of throttle in hydraulic feedback
$M_{x,i}$	Swash plate torque load of piston $i$
$P_{Loss}$	Power loss
$p_{HP}$	Pressure at high pressure port
$p_A$	Pressure of control actuator
$p_i$	Piston pressure of piston $i$
$Q_{Bypass}$	Flow rate of bypass orifice
$Q_{MF}$	Flow rate of damper cylinder
$R$	Pitch radius
$s_i$	Piston stroke of piston $i$
$T_S$	Settling time
$V_{HF}$	Volume of cylinder in hydraulic feedback
$x_C$	Stroke of control actuator
$x_D$	Stroke of damper in mechanical feedback
$x_{PCV}$	Stroke of pressure control valve
$\alpha$	Area ratio of control actuator
$\alpha_D$	Flow rate coefficient
$\beta$	Swash plate angle
$\eta$	Dynamic viscosity of the oil
$\rho$	Density
$\varphi_i$	Rotational angle of piston $i$

## REFERENCES

- [1] Dreytmüller J (1975) Hydraulisch-mechanische Druckregelung an verstellbaren Axialkolbenpumpen. Dissertation, RWTH Aachen University
- [2] Murrenhoff H (1983) Regelung von Verdrängereinheiten am Konstant-Drucknetz. Dissertation, RWTH Aachen University
- [3] Langen A (1986) Experimentelle und analytische Untersuchungen an vorgesteuerten hydraulisch-mechanischen und elektrohydraulischen Pumpenregelungen. Dissertation, RWTH Aachen University
- [4] Manring ND, Johnson RE (1996) Modeling and Designing a Variable-Displacement Open-Loop Pump. *Journal of Dynamic Systems, Measurement, and Control* 118(2): 267-271
- [5] Manring ND (1999) The Control and Containment Forces on the Swash Plate of an Axial Piston Pump. *Journal of Dynamic Systems, Measurement, and Control* 121(4): 599-605
- [6] Mandal NP et al (2013) Pressure Compensator Design for a Swash Plate Axial Piston Pump. *Journal of Dynamic Systems, Measurement, and Control* 136(2)
- [7] Lux J, Murrenhoff H (2016) Experimental loss analysis of displacement controlled pumps. In: 10th International Fluid Power Conference Proceedings, Dresden, 8-10 March 2016
- [8] Schoemacker F, Murrenhoff H (2019) Interaction between Swash Plate Movement and Commutation in Axial Piston Machines. *JFPS Journal of Fluid Power Systems* 11(3): 49-54
- [9] Murrenhoff H (2012) Servohydraulik- Geregelt hydraulische Antriebe. Shaker Verlag, Aachen
- [10] Luhmer H (1981) Aufbau hydraulischer Netzwerke mit differenzierendem Verhalten und ihr Einsatz zur Dämpfung hydrostatischer Antriebe. Dissertation, RWTH Aachen University
- [11] Weingarten F (1983) Aufbau hydraulischer Zeitglieder und ihr Einsatz im Signalzweig hydraulisch-mechanischer Regelungen. Dissertation, RWTH Aachen University
- [12] Keviczky L et. al (2019) Control Engineering. Springer Nature Singapore Pte Ltd., Singapore